Calcite Structure

DOI: 10.1002/anie.200603327

Local Atomic Order and Infrared Spectra of Biogenic Calcite**

*Rachel Gueta, Amir Natan, Lia Addadi, Steve Weiner, Keith Refson, and Leeor Kronik**

Calcite and aragonite are among the most common minerals in natural biomaterials.[1] Almost all organisms control the type of calcium carbonate polymorph formed, the crystal morphology, and the ultrastructural organization. During biogenic calcium carbonate formation in certain species from several major phyla, a transient disordered phase, called amorphous calcium carbonate (ACC), is initially produced. It subsequently transforms into either calcite or aragonite.[2] Furthermore, the transient ACC phase assumes the local order (around calcium ions) of the stable phase into which it transforms.[3,4] Interestingly, in sea urchin larval spicules, even when the forming spicule is composed of about 80% ACC, the amount of H_2O is only about 1% by weight.[5]

Infrared (IR) spectroscopy of minerals provides key information not only on polymorph type, but also on the extent of atomic order.[6] In calcite, three major IR absorption peaks are identified: ν_3 (an asymmetric stretch), ν_2, and ν_4. The last two correspond to out-of-plane and in-plane bending vibrations of the carbonate ions, respectively.[7] Beniash et al.[8] found that the ν_2/ν_4 peak intensity ratio of the mineral forming the larval spicule of the sea urchin *Paracentrotus lividus* varies significantly with spicule development. The ν_4 peak becomes sharper, whereas the ν_2 peak remains essentially constant, and thus the ν_2/ν_4 intensity ratio decreases from about 10 to about 3; the latter value is typical of nonbiogenic calcite. These variations correlate with changes in the intensity per unit volume of the major X-ray diffraction peak of calcite.[8] These observations were attributed to initial deposition of ACC that subsequently crystallized into a single crystal of calcite. Thus, the more crystalline the mineral, the lower the ν_2/ν_4 intensity ratio. Despite the fact that the deposition of transient ACC is now known to be an important strategy in biomineralization,[9] no explanation for the dependence of the IR spectrum of calcite on crystalline order has emerged. Here we provide such an explanation by computing phonon (lattice vibration) spectra for ideal and distorted calcite unit cells from first-principles quantum mechanical calculations using density functional theory (DFT).[10]

Irrespective of the computational method, a major difficulty is the need to model vibrations in an amorphous material, in which some bond lengths and angles may be somewhat larger than their equilibrium value, whereas others may be somewhat shorter. These local distortions nearly preserve the short-range order, but the lack of register between adjacent local units destroys long-range order. However, if ν_2 and ν_4 are due to relatively dispersion free optical phonons (an assumption confirmed below), they are insensitive to long-range order. Hence, it is possible to consider the vibrational spectrum in slightly distorted crystalline structures. The experimental IR spectra would then correspond to an average of vibrational spectra over an ensemble of locally distorted crystalline structures.

Ideally crystalline calcite was constructed with a rhombohedral unit cell (Figure 1). All structural and vibrational properties were computed by solving the Kohn–Sham equations within the local density approximation (LDA)[10] on a plane-wave basis[11] by using CASTEP.[12] In particular, phonon dispersion curves were computed by using the recently implemented density functional perturbation theory formalism.[13] Norm-conserving pseudopotentials[14] were used throughout. A *k*-point grid containing 28 points

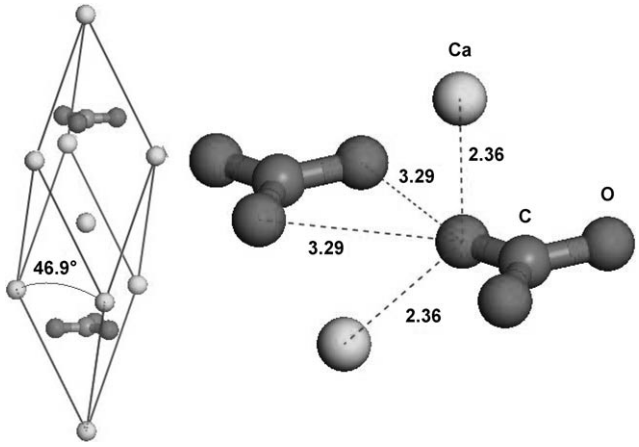

Figure 1. Left: Ideal calcite structure showing the rhombohedral angle. Right: Enlargement of the environment of one O atom showing the ideal nearest-neighbor Ca–O distance (2.36 Å) and $O^1\cdots O^2$ distance (3.29 Å) for the ideal structure.

[*] A. Natan,[+] Dr. L. Kronik
Department of Materials and Interfaces
Weizmann Institute of Science
Rehovoth 76100 (Israel)
Fax: (+972) 8-934-4138
E-mail: leeor.kronik@weizmann.ac.il
R. Gueta,[+] Prof. L. Addadi, Prof. S. Weiner
Department of Structural Biology
Weizmann Institute of Science
Rehovoth 76100 (Israel)
Dr. K. Refson
Rutherford Appleton Laboratory
Chilton, Didcot
Oxfordshire OX11 0QX (UK)

[+] These authors contributed equally to this work.

[**] L.K., L.A., and S.W. are the incumbents of the Delta career development chair, the Dorothy and Patrick Gorman professorial chair of biological ultrastructure, and the Dr. Trude Burchardt professorial chair of structural biology, respectively. This work was supported in part by the Minerva Foundation.

Supporting information for this article is available on the WWW under http://www.angewandte.org or from the author.

in the irreducible Brillouin zone and a cutoff energy of 73 Ry were found to be sufficient for convergence.[15] All forces were relaxed to better than 0.002 eV Å^{-1}.

Force and stress relaxation resulted in theoretical equilibrium lattice parameter and rhombohedral angle of $a=$ 6.28 Å and $\alpha=46.9°$, respectively, which translates into $a=$ 5.00 Å and $c=16.74$ Å for the hexagonal unit-cell representation. These values are in good agreement with the experimental values of $a=4.99$ Å and $c=17.06$ Å,[16] with residual error typical of LDA calculations. This validates our choice of both functional and pseudopotentials as sufficiently accurate for the present problem. Further validation was obtained by computing the phonon dispersion curve along the [111] direction and comparing it to the neutron-scattering data of Cowley and Pant[17] (Figure 2). Qualitative agreement between experiment and theory is found throughout. Quantitative agreement is never worse than about 30 cm^{-1} and is usually substantially better.

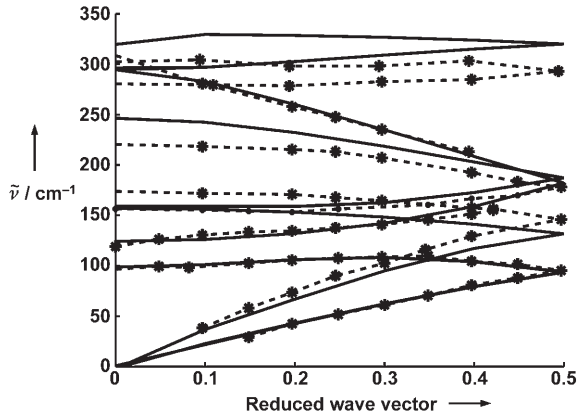

Figure 2. Comparison between theoretical and experimental phonon dispersion spectra of ideal calcite along the [111] direction. Solid lines: DFT calculation. Dashed lines: neutron-scattering data.[17] Symbols denote actual experimental data points. Theoretical higher energy phonon spectra that are outside the range of the experimental dispersion data are given in the Supporting Information.

Significantly, quantitative agreement between theory and experiment was found for both ν_2 and ν_4 of ideal calcite. In-plane bending vibrations of the carbonate ions were found theoretically at 713, 714, and 716 cm^{-1}, in excellent agreement with the experimental $\tilde{\nu}_4$ value of 713 cm^{-1}. Out-of-plane bending vibrations were found theoretically at 871 and 880 cm^{-1}, in excellent agreement with the experimental $\tilde{\nu}_2$ value of 875 cm^{-1}.[18] Particularly notable was the absence of meaningful dispersion for these frequencies (ca. 0 for $\tilde{\nu}_4$ and ± 5 cm^{-1} for $\tilde{\nu}_2$, see the Supporting Information), which justifies our distorted-cell approach.

Distorted structures were generated by altering the rhombohedral angle and subsequently allowing all atoms within the unit cell to relax, creating a strained lattice. We emphasize that this does not necessarily imply a macroscopic strain in the real material, because the overall strain averages to zero in a distribution of locally distorted unit cells, with distortions occurring in opposite directions. The rhombohedral angle was changed from its equilibrium value of 46.9° to values of 44, 45.5, 46.2, 47.7, 48.5, and 50°. Because relaxation preserved the symmetry of the system, the carbonate groups remained coplanar. The deformation induced nearly negligible changes in the C–O distance (0.005–0.01 Å), but more sizable variations in the Ca–O (0.05–0.1 Å) and $O_{(carbonate1)}\cdots O_{(carbonate2)}$ distances (0.15–0.3 Å) (Figure 1). Both the Ca–O and the $O^1\cdots O^2$ distance were found to depend linearly on the angle. A summary[19] of ν_2 and ν_4 vibrational frequencies (computed only at the Gamma point, as appropriate for IR spectroscopy) as a function of the relaxed Ca–O distances is given in Figure 3. For small deviations, both $\tilde{\nu}_2$ and $\tilde{\nu}_4$ depend linearly on the Ca–O and $O^1\cdots O^2$ distances, but the change in $\tilde{\nu}_4$ is clearly much larger than that of $\tilde{\nu}_2$ for all tested deformations.

Assuming that an amorphous material is characterized by a distribution of unit cells with varying distortion, we now understand why the ν_2/ν_4 peak intensity ratio is order-dependent. With decreasing order, variation in the Ca–O and $O^1\cdots O^2$ distances is greater. This, in principle, will cause both the ν_2 and ν_4 peaks to broaden and diminish their peak heights. However, Figure 3 shows that this effect is much more pronounced for ν_4, and hence the ν_2/ν_4 ratio increases. This can also be made semiquantitative. Suppose that both peaks have a natural width σ and that the Ca–O (or $O^1\cdots O^2$) distance has a distribution of width σ_d (d is the Ca–O or $O^1\cdots O^2$ distance). Using elementary random variable theory assuming Gaussian distributions, we readily obtain a ν_2/ν_4 peak intensity ratio proportional to $\sqrt{(\sigma^2+a_{\nu_4}^2\sigma_d^2)/(\sigma^2+a_{\nu_2}^2\sigma_d^2)}$, in which a_{ν_4} and a_{ν_2} are the slopes of the vibration versus Ca–O (or $O^1\cdots O^2$) distance curves of Figure 3 a and b, respectively. This relation is plotted in Figure 3 c, with $\sigma=5$ cm^{-1} and the proportionality constant set to 3 to agree with the experimental peak intensity ratio in the ideal crystalline case ($\sigma_d=0$ Å). It shows that peak intensity ratios vary from 3 for the ideal crystal to 10 for a highly disordered one. The extent to which this prediction agrees with experiment is visualized in Figure 4. It shows several theoretical spectra obtained by broadening the ideal frequencies with different values of σ_d (0, 0.03, 0.1 Å) in comparison with experimental results. Clearly, even though the theory is based on very simple assumptions, it is in qualitative and even semiquantitative agreement with experiment.

We now consider why the ν_4 mode is more sensitive than the ν_2 mode to the relative positions Ca–O and $O^1\cdots O^2$. As the Ca–O and $O^1\cdots O^2$ distances change, so does the potential landscape "viewed" by the carbonate group. This, in turn, changes the effective "spring constants" for both ν_2 and ν_4. While the direction of the Ca–O bonds is not orthogonal to either the ν_2 or the ν_4 vibration, it can be shown that the fluctuation of the Ca–O distance during vibration is three times larger for the ν_4 mode than for the ν_2 mode. This can explain phenomenologically why the ν_4 mode is more sensitive to changes in the Ca–O distance. As for the $O^1\cdots O^2$ distance, the difference in carbonate–carbonate distance (which it represents) affects the in-plane bending vibration ν_4 more than the out-of-plane bending vibration ν_2, simply because the carbonate moieties are coplanar. The

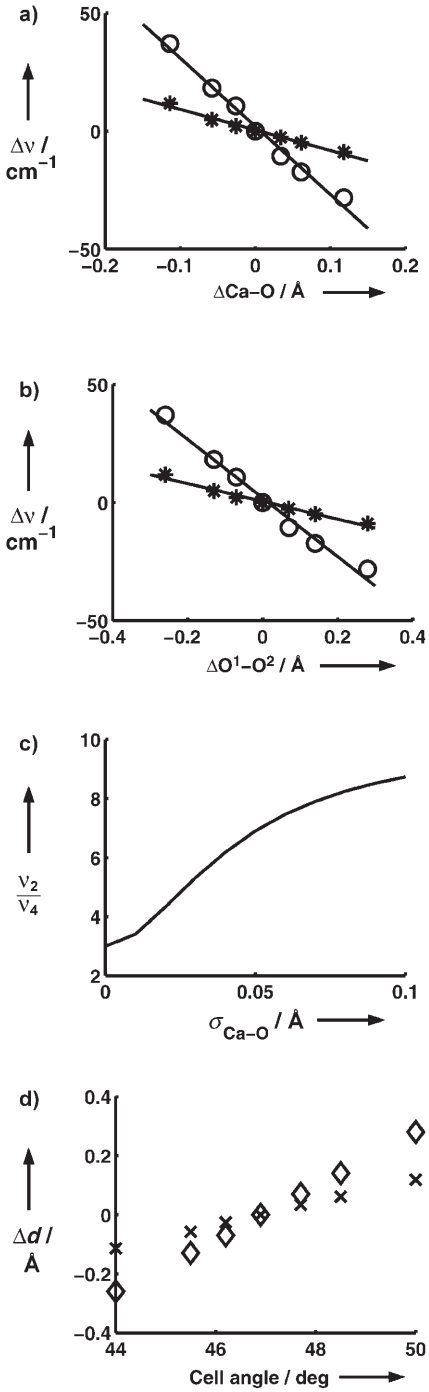

Figure 3. a) Changes in ν_4 (circles) and ν_2 (asterisks) vibrational frequencies as a function of Ca–O distance change. b) Changes in ν_4 (circles) and ν_2 (asterisks) vibrational frequency as a function of the $O^1\cdots O^2$ distance change. c) Predicted ν_2/ν_4 peak intensity ratio as a function of σ_d (d is the Ca–O distance). d) Changes in Ca–O (crosses) and $O^1\cdots O^2$ (diamonds) distances as a function of the rhombohedral cell angle.

$O^1\cdots O^2$ distance is much larger than the Ca–O distance, but so also is the extent to which it shrinks as a function of the distortion applied (9 versus 5%, respectively, as shown in Figure 3d).

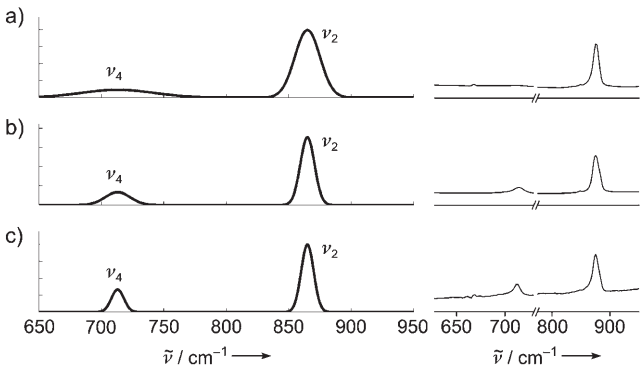

Figure 4. Comparison of simulated (left) and experimental (right) IR spectra. a) 100% transient amorphous calcite and a simulated spectrum with $\sigma_d = 0.1$ Å (d is the Ca–O distance). b) 80–90% transient amorphous calcite and a simulated spectrum with $\sigma_d = 0.03$ Å; c) Geological calcite and the ideal theoretical spectrum ($\sigma_d = 0$ Å). Experimental data are taken from reference [3].

These results elucidate the basis for the changes in IR spectra observed during the transformation of ACC into calcite. We note that we have not considered the possible contribution of occluded water to the IR spectrum, because in the transient ACC of forming sea urchin larval spicules water is essentially absent.[5] In contrast, stable biogenic ACC[2] and synthetic ACC[20,21] do contain water and this may further affect their IR spectra. We also note that in the transformation from ACC to aragonite an opposite trend is observed experimentally,[22] and that there are consistent differences in ν_2/ν_4 peak intensity ratio between shell layers with different ultrastructures in an adult aragonitic mollusk shell.[23] Furthermore, calcites produced by heating calcium carbonate to high temperature (to produce plaster and mortar) and then allowing the CaO to hydrate and absorb CO_2 from the atmosphere also have different ν_2/ν_4 peak intensity ratios. Although these phenomena are almost certainly different in terms of the produced atomic disorder compared to that we have investigated here, they do show that lattice distortions are preserved even in the mature stable calcium carbonate polymorphs and, significantly, appear to reflect the mode by which they formed. This opens up exciting possibilities for identifying calcites produced under different conditions, and of better understanding ways in which they form. This may well have applications not only in the field of biomineralization, but also in geology, archaeology, and in the materials sciences.

Received: August 15, 2006
Published online: November 24, 2006

Keywords: bioinorganic chemistry · calcite · calcium · density functional calculations · vibrational spectroscopy

[1] H. A. Lowenstam, S. Weiner, *On Biomineralization*, Oxford University Press, New York, **1989**.
[2] L. Addadi, S. Raz, S. Weiner, *Adv. Mater.* **2003**, *15*, 959.
[3] Y. Politi, Y. Levi-Kalisman, S. Raz, F. Wilt, L. Addadi, S. Weiner, I. Sagi, *Adv. Funct. Mater.* **2006**, *16*, 1289.

[4] B. Hasse, H. Ehrenberg, J. Marxen, W. Becker, M. Epple, *Chem. Eur. J.* **2000**, *6*, 3679.
[5] S. Raz, P. C. Hamilton, F. H. Wilt, S. Weiner, L. Addadi, *Adv. Funct. Mater.* **2003**, *13*, 480.
[6] V. C. Farmer, *The Infrared Spectra of Minerals*, Mineralogical Society, London, **1974**.
[7] W. B. White in *The Infrared Spectra of Minerals* (Ed.: V. C. Farmer), Mineralogical Society, London, **1974**, chap. 12, p. 227.
[8] E. Beniash, J. Aizenberg, L. Addadi, S. Weiner, *Proc. R. Soc. London Ser. B* **1997**, *264*, 461.
[9] S. Weiner, I. Sagi, L. Addadi, *Science* **2005**, *309*, 1027.
[10] W. Koch, M. C. Holthausen, *A Chemist's Guide to Density Functional Theory*, 2nd ed., Wiley-VCH, Weinheim, **2001**.
[11] J. Ihm, A. Zunger, M. L. Cohen, *J. Phys. C* **1979**, *12*, 4409.
[12] M. D. Segall, P. L. D. Lindan, M. J. Probert, C. J. Pickard, P. J. Hasnip, S. J. Clark, M. C. Payne, *J. Phys.: Cond. Matt.* **2002**, *14*, 2717; S. J. Clark, M. D. Segall, C. J. Pickard, P. J. Hasnip, M. J. Probert, K. Refson, M. C. Payne, *Z. Kristallogr.* **2005**, *220*, 567.
[13] K. Refson, P. R. Tulip, S. J. Clark, *Phys. Rev. B* **2006**, *73*, 155114.
[14] Optimized pseudopotentials with kinetic energy filter tuning were used (M.-H. Lee, PhD Thesis, University of Cambridge, **1995**; available online at http://boson4.phys.tku.edu.tw/qc/my_thesis/). Numerical details are given in the Supporting Information.
[15] Using a larger *k*-point grid containing 63 points in the irreucible Brillouin zone yielded a change of about 0.1 cm^{-1} in $\tilde{\nu}_2$ and $\tilde{\nu}_4$ and a maximal change of 1.5 cm^{-1} over all frequencies. Using a finer FFT grid yielded a change of 0.2 cm^{-1} in $\tilde{\nu}_2$, 0.04 cm^{-1} for $\tilde{\nu}_4$, and 1.5 cm^{-1} over all frequencies.
[16] R. W. G. Wyckoff, *Crystal Structures*, 2nd ed., Interscience, New York, **1963**.
[17] E. R. Cowley, A. K. Pant, *Phys. Rev. B* **1973**, *8*, 4795.
[18] The values reported are Gamma point values along the (111) direction. For the ν_2 mode, they differ slightly from those along the (100) direction, for which values of 865 and 871 cm^{-1} were obtained. This is due to the splitting of longitudinal and transverse optical phonons [see, e.g., C. M. Wolfe, N. Holonyak, Jr., G. E. Stillman, *Physical Properties of Semiconductors*, Prentice Hall, Englewood Cliffs, **1989**]. All $\tilde{\nu}_2$ values reported here are for the (111) direction. For completeness, the entire analysis was also performed along the (100) direction with the same conclusions. The latter analysis is given in the Supporting Information.
[19] Because there is more than one value for $\tilde{\nu}_4$ and for $\tilde{\nu}_2$, the value exhibiting maximal deviation for each mode is the one shown. The complete data appear in the Supporting Information.
[20] M. Faatz, F. Gröhn, G. Wegner, *Adv. Mater.* **2004**, *16*, 996; M. Faatz, F. Gröhn, G. Wegner, *Mater. Sci. Eng. C* **2005**, *25*, 153.
[21] M. M. Tlili, M. Ben Amor, C. Gabrielli, S. Joiret, G. Maurin, P. Rousseau, *J. Raman Spectrosc.* **2001**, *33*, 10.
[22] I. M. Weiss, N. Tuross, L. Addadi, S. Weiner, *J. Exp. Zool.* **2002**, *293*, 478.
[23] R. Gueta, MSc Thesis, Weizmann Institute of Science **2005**.

